Check for updates

Impact of various dopant elements on the electronic structure of Cu$_2$ZnSnS$_4$ (CZTS) thin films: a DFT study

Andrey A. Kistanov, [iD] *[a] Wei Cao, [iD] [a] Marko Huttula,[a] Salavat Kh. Khadiullin,[b] Elena A. Korznikova,[c] Aliaksandr Smirnov,[d] Xinghui Wang[e] and Siarhei Zhuk[d]

New structures made based on Cu$_2$ZnSnS$_4$ (CZTS) by substitutions with Cr, Ti, V, and Mo species were investigated *via* density functional theory. The total substitution of Zn by Cr and V leads to the vanishing of the bandgap, while n-type conductivity with a low bandgap of 0.19 eV was predicted in the case Ti. In addition, the conduction band minimum and valence band maximum overlapping were observed for the Mo/Sn ratio of 1/3. Therefore, our study suggests that even the low content of alternative cations in CZTS allows to control its band alignment. The obtained results can be helpful for designing CZTS-based intermediate layers to improve the quality of the back interface of the CZTS thin-film solar cells.

Introduction

Cu$_2$ZnSnS$_4$ (CZTS) thin films have attracted considerable interest in the last decade due to their high potential for the application in photovoltaics.[1,2] Suitable optical and electronic properties make CZTS a promising photovoltaic material for the thin-film solar cells.[3] The CZTS thin films are characterized by a moderate direct bandgap of 1.5 eV and high absorption coefficient ($>10^4$ cm^{-1}) making them interesting candidates for single-junction solar cells.[4] Moreover, CZTS possesses intrinsic p-type conductivity due to the presence of Cu vacancies that form shallow acceptor levels.[5] In addition, the bandgap of CZTS can be modulated in the range from 1 to 1.5 eV by tuning S/(Se + S) ratio from 0 to 1.[6] Furthermore, CZTS thin films demonstrate electronic properties comparable to those of Cu(In, Ga)Se$_2$ (CIGS) films.[1] The latter are widely used in the commercial fabrication of highly efficient thin-film solar cells. In contrast to CIGS, rare-earth elements, In and Ga, are replaced with abundant Zn and Sn in CZTS. The highest reported power conversion efficiency (PCE) for CZTSSe solar cells is 12.6%.[7]

On the other hand, champion CIGS and CdTe thin-film solar cells demonstrate PCE of 23.35% and 22.2%, respectively.[8] The lack of improvement in the performance of kesterite solar cells is attributed to the defect intolerant nature of the photovoltaic (PV) material.[9] The formation of various anti-site defects and clusters of defects is reported for the complex quaternary compound system.[10] These defect centers contribute to the recombination and result in low open-circuit voltage (V_{oc}) of kesterite solar cells, which is known to be a major bottleneck limiting the device performance. Moreover, cation-disordering causing the recombination is associated with similar size of cations constituting CZTS.[11] Replacing a cation with an isovalent cation of different size is an effective way to suppress the defect formation and reduce the V_{oc} deficit of kesterite solar cells.[12] Recent progress in the cation substitution is systematically reviewed in the work of Li *et al.*[13] The incorporation of Ag caused an increase in the bandgap and decrease of carrier concentration.[14] The reduced concentration of Ag, in turn, led to an increase in the width of the depletion region.

For CZTS, it has been found that the partial substitution of Zn by Cd causes a decrease in its bandgap and enhancement of the minority carrier lifetime.[15,16] Moreover, the Cd substitution allows the fabrication of highly efficient pure sulfide kesterite solar cells prepared using the sputtering and solution-based approach.[17] However, the addition of toxic Cd into non-toxic CZTS may limit its application perspectives because of the environmental concern. Another study by Kumar *et al.* focused on the review of Zn substitution in CZTS.[18] Alternatives to Cd such as Mn, Fe, Co, Ni and Ba are examined in the study in detail.

Obviously, experimental brute force methods of searching for the best substituents are expensive, requiring significant

[a] *Nano and Molecular Systems Research Unit, University of Oulu, 90014 Oulu, Finland. E-mail: andrey.kistanov@oulu.fi*
[b] *Ufa State Aviation Technical University, 450000 Ufa, Russia*
[c] *Institute for Metals Superplasticity Problems, Russian Academy of Sciences, 450001 Ufa, Russia*
[d] *Belarusian State University of Informatics and Radioelectronics, 220013 Minsk, Belarus*
[e] *College of Physics and Information Engineering, Institute of Micro-Nano Devices and Solar Cells, Fuzhou University, Fuzhou 350108, China*

labor inputs, and are time-consuming. To suggest the optimal substituents and speed up the progress in the synthesis of high-quality kesterite thin films, atomic simulations are required. The density functional theory (DFT) is the most popular approach in solid-state physics as this method is able to predict the electronic properties of a solid with an excellent ratio of accuracy and computational demand.[19–21]

In contrast to the above-mentioned studies, which aims to find suitable cation substitution approaches to fabricate CZTS absorber layers of higher quality, the present study demonstrates a way to develop the CZTS-based intermediate layer. CZTS is known for its instability when in contact with Mo at high processing temperatures.[22] Detrimental solid-state reactions at the rear contact lead to the void formation due to the evaporation of volatile secondary phases.[5,22] Furthermore, the loss of Zn and Sn occurs during sulfurization.[5] In addition, voids are reported to increase the series resistance of CZTS solar cells.[23] Therefore, ILs are deposited to suppress the reaction at the interface between Mo and CZTS.[24] However, the insertion of an IL may lead to the degradation of CZTS crystallinity as the crystal structures of the materials are different.[25]

In this work, we use first-principles DFT simulations to study the effect of Zn substitution by Cr, Ti, and V. These elements were chosen for the substitution as they are characterized by a significantly higher melting temperature relative to that of Zn with the oxidation state of +2. To the best of our knowledge, no studies on simulation of Cu_2-$CrSnS_4$, Cu_2TiSnS_4 and Cu_2VSnS_4 are reported to date. In addition, in a recent report, we demonstrated a remarkable improvement in the PCE of sputtered CZTS solar cells from 1.6% to 5.5% owing to the Mo incorporation.[26] Since evidence of Sn substitution by Mo were observed, in this study, we also investigate the effect of the partial substitution of Sn by Mo on the energy bands distribution using DFT simulations to provide insights enabling more efficient designing of CZTS based absorbers.

Methods

The DFT based first-principles calculations were performed using the plane-wave Vienna *ab initio* simulation package (VASP).[27] The Perdew–Burke–Ernzerhof (PBE) exchange–correlation functional under the generalized gradient approximation[28] (GGA) together with the van der Waals corrected functional with Becke88 optimization[29] were used for geometry optimization of all structures and band structure calculations of strained Cu_2TiSnS_4. The electronic structure of the structures with the full substitution of Zn/Sn was considered using the accurate hybrid functional (HSE06). Due to the high computational cost of hybrid functionals, the electronic structure of all the remaining structures (with the partial substitution) was considered using PBE GGA. All the structures are fully relaxed until the atomic forces and total energy values were smaller than 0.01 eV Å^{-1} and 10^{-6} eV,

respectively. The kinetic energy cutoff of 400 eV was adopted. Periodic boundary conditions were applied in all three directions. The first Brillouin zone was sampled with a 15 × 15 × 8 k-mesh grid. The Mo/Sn ratio was controlled by the substitution of the Sn by Mo atoms.

The calculated lattice constants a (b) and c of the considered pure CZTS unit cell (see Fig. 1a) were found to be 5.435 Å and 10.843 Å, respectively. Our results are well compared with experimental[30] and theoretical data.[31–33] The bandgap size (1.38 eV) calculations for pure CZTS (see Fig. 1b) show high accuracy and are comparable with the theoretical and experimental data (1.4–1.5 eV) reported in a number of works.[34–36]

Results and discussion

Firstly, the effect of the partial substitution of Zn by Cr, Ti, and V is considered. Fig. 2a–c show the band (bottom panel) and the atomic (top panel) structures of CZTS with Zn atoms substituted by Cr, Ti, and V atoms, respectively. The study shows the presence of Cr (see Fig. 2a) that leads to the downward shift of the conduction band minimum (CBM) and the upward shift of valance band maximum (VBM). The CBM crosses the Fermi level at the point between Γ and X points, and VBM crosses the Fermi level at the point between nearby the N point, which evidences the closing of the Cu_2-$CrSnS_4$ bandgap. It should be noted that the partial substitution of Zn by Cr (at the Cr/Zn ratio of 1/1) also leads to the closing of the bandgap (see Fig. 3a). The modification of the CZTS bandgap with the incorporation of Cr was also observed in the experimental study.[37] The addition of Cr in CZTS was carried out by the co-sputtering of CZTS and Cr targets. It has been reported that the incorporation of Cr into CZTS performed by the co-sputtering of CZTS and Cr targets modified the bandgap and structural properties of CZTS thin films. With the increase of Cr content from 0 to ~9%, the bandgap increased from 1.51 eV to 1.7 eV. On the other hand, the bandgap decreased to 1.54 eV when measured Cr was ~15.8%. Note, that in contrast to the study of Sapeli *et al.*,
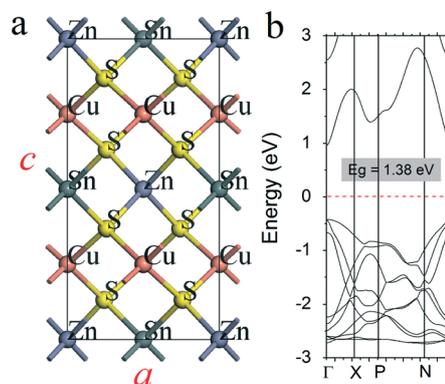

Fig. 1 Atomic configuration (a) and band structure (HSE06) (b) of CZTS. The red dashed line represents the Fermi level.
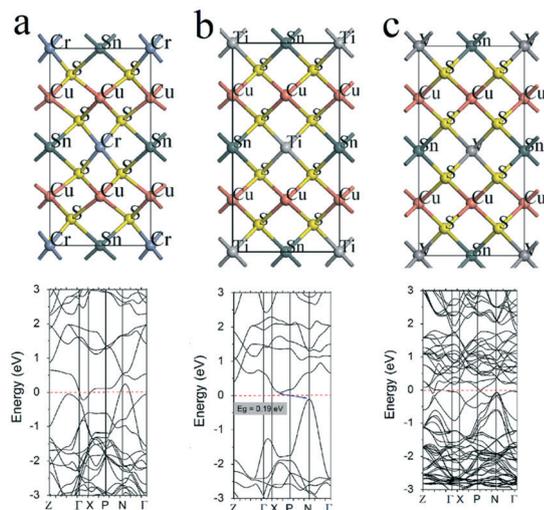
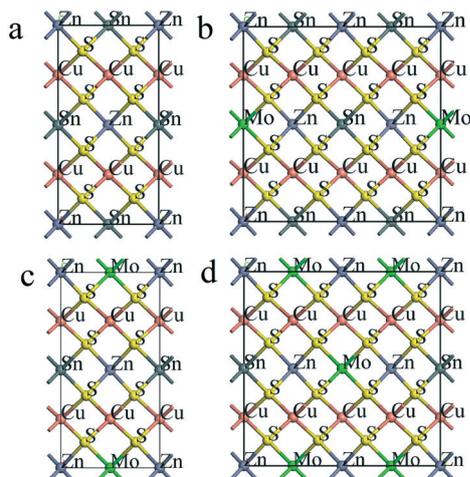**Fig. 4** Atomic configuration of Mo-doped CZTS for the Mo/Sn ratio of (a) 0, (b) 1/3, (c) 1/1 and (d) 3/1. The Cu, Zn, Sn, S, and Mo atoms are colored in red, violet, gray, yellow and green, respectively.
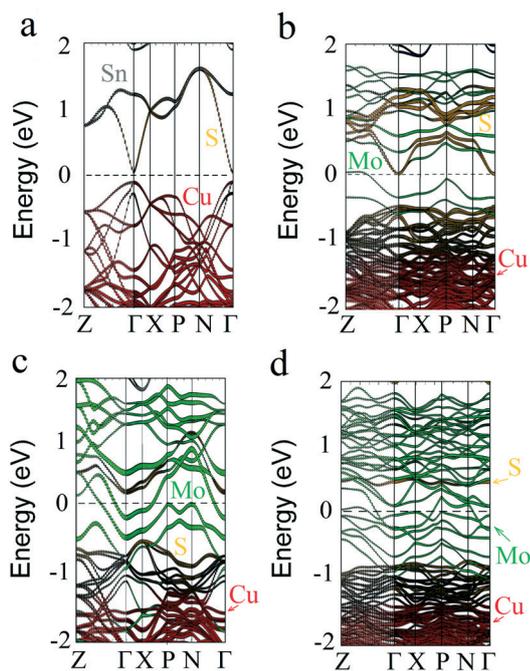

Fig. 5 Band structure (GGA PBE) of Mo-doped CZTS for the Mo/Sn ratio of (a) 0, (b) 1/3, (c) 1/1 and (d) 3/1. The bands corresponding to Cu, Zn, Sn, S, and Mo atoms are colored in red, violet, gray, yellow and green, respectively. The horizontal black line represents the Fermi level.

Fig. 6 LDOS of Mo-doped CZTS for the Mo/Sn ratio of (a) 0, (b) 1/3, (c) 1/1 and (d) 3/1. The bands corresponding to Cu, Zn, Sn, S, and Mo atoms are colored in red, violet, gray, yellow and green, respectively. The vertical black lines represent the Fermi level.

To deeply understand changes taking place within the energy gap of CZTS upon Mo doping, the local density of states (LDOS) analysis of pristine and Mo-doped CZTS was also conducted (see Fig. 6). As shown in Fig. 6b, at the Mo/Sn ratio of 1/3, Mo states are significantly broadened and strongly mixed with the states of the host material. In addition, the upward shift of Sn states is observed. An increase of Mo concentration leads to the further shift of Sn states and the appearance of Mo states within the energy

gap. Importantly, the spin splitting and broadening of Mo states increase with the increasing concentration (see Fig. 6c and d). An interesting feature of Mo-doped CZTS is that only spin up states (all are Mo states) are occupied below the Fermi level, which may be responsible for its enhanced light-harvesting ability.

Using interpolation of the results we may expect the existence of the bandgap for CZTS with the Mo/Sn ratio in the range from 0 to 1/3. Formation of metallic-like CZTS supports observed reduction in resistivity of the CZTS thin films as a result of Mo incorporation in our recent experimental work.[26] In addition, this may also explain the

enhanced fill factor of Mo-incorporated CZTS solar cells by the formation of better ohmic contact at the CZTS/Mo interface.

The simulation data presented in Fig. 6 provides an additional explanation of the phenomena of the increased light absorbance for Mo-incorporated CZTS thin films reported in our experimental study.[26] Given the short minority charge carrier diffusion length in CZTS,[38] the fabrication of the solar cells with an ultrathin absorber layer is useful to enhance charge collection efficiency. Therefore, the improvement of light absorption in CZTS thin films *via* the alternative cation incorporation is critical for the ultrathin absorber layer to maintain the harvesting of a reasonable portion of incident photons. For this reason, it may contribute to the overall improvement of CZTS solar cell performance. In addition, improved understanding of the nature of the increase in the conductivity of Mo-substituted CZTS thin films, allows the designing of CZTS solar cells with a back surface field where Mo-substituted CZTS is used as IL to reduce recombination at the back interface and improve charge transport.[39]

Conclusions

The study demonstrated that new compounds such as Cu_2CrSnS_4, Cu_2TiSnS_4, Cu_2VSnS_4 and $Cu_2Zn(Sn_x,Mo_{1-x})S_4$ can be formed. It has been revealed that the full substitution of Zn in CZTS results in the closing of the bandgap for the case of Cu_2CrSnS_4 and Cu_2VSnS_4, while the overlapping of CBM and VBM was observed at the Mo/Sn ratio of 1/3. In addition, n-type Cu_2CrSnS_4 with a low bandgap of 0.19 eV was simulated. This study shows that the relatively low content of alternative cations in the CZTS absorber layer significantly affects the distribution of energy levels in conduction and valence bands, thus providing additional ways to control band alignment.

The obtained results can be useful for designing CZTS solar cells with IL based on the same crystal structure. First, highly conductive Cu_2CrSnS_4, Cu_2VSnS_4 and $Cu_2Zn(Sn_x, Mo_{1-x})S_4$ ILs can be used to improve the ohmic properties of the back contact. In addition, these IL may address the problem of the increased series resistance of the solar cells due to the presence of voids at the back interface. Second, since these new compounds exhibit the same crystal structure as CZTS, they can be used as a seed layer to facilitate the growth of high-quality CZTS absorber layer. Third, the substitution of Zn and Sn by elements with much higher melting temperatures may suppress its loss from the CZTS absorber layer during high-temperature sulfurization as the elemental loss causes the formation of anti-site defects and vacancies.

Conflicts of interest

There are no conflicts to declare.

References

1 X. Liu, Y. Feng, H. Cui, F. Liu, X. Hao, G. Conibeer, D. B. Mitzi and M. Green, *Prog. Photovolt: Res. Appl.*, 2016, **24**, 879–898.

2 S. A. Khalate, R. S. Kate and R. J. Deokate, *Sol. Energy*, 2018, **169**, 616–633.

3 K. Ito, *Copper zinc tin sulfide-based thin-film solar cells*, Wiley, Chichester, 2015.

4 D. B. Mitzi, O. Gunawan, T. K. Todorov, K. Wang and S. Guha, *Sol. Energy Mater. Sol. Cells*, 2011, **95**, 1421–1436.

5 M. Kumar, A. Dubey, N. Adhikari, S. Venkatesan and Q. Qiao, *Energy Environ. Sci.*, 2015, **8**, 3134–3159.

6 J. He, L. Sun, S. Chen, Y. Chen, P. Yang and J. Chu, *J. Alloys Compd.*, 2012, **511**, 129–132.

7 W. Wang, M. T. Winkler, O. Gunawan, T. Gokmen, T. K. Todorov, Y. Zhu and D. B. Mitzi, *Adv. Energy Mater.*, 2014, **4**, 1–5.

8 M. A. Green, E. D. Dunlop, D. H. Levi, J. Hohl-Ebinger, M. Yoshita and A. W. Y. Ho-Baillie, *Prog. Photovoltaics*, 2019, **27**, 565–575.

9 S. Siebentritt, *Thin Solid Films*, 2013, **535**, 1–4.

10 S. Chen, A. Walsh, X. G. Gong and S. H. Wei, *Adv. Mater.*, 2013, **25**, 1522–1539.

11 S. Bourdais, C. Choné, B. Delatouche, A. Jacob, G. Larramona, C. Moisan, A. Lafond, F. Donatini, G. Rey, S. Siebentritt, A. Walsh and G. Dennler, *Adv. Energy Mater.*, 2016, **6**, 1502276.

12 C. Yan, K. Sun, J. Huang, S. Johnston, F. Liu, B. P. Veettil, K. Sun, A. Pu, F. Zhou, J. A. Stride, M. A. Green and X. Hao, *ACS Energy Lett.*, 2017, **2**, 930–936.

13 J. Li, D. Wang, X. Li, Y. Zeng and Y. Zhang, *Adv. Sci.*, 2018, **5**, 1700744.

14 A. Guchhait, Z. Su, Y. F. Tay, S. Shukla, W. Li, S. W. Leow, J. M. R. Tan, S. Lie, O. Gunawan and L. H. Wong, *ACS Energy Lett.*, 2016, **1**, 1256–1261.

15 Z. Su, J. Ming, R. Tan, X. Li, X. Zeng, S. K. Batabyal and L. H. Wong, *Adv. Energy Mater.*, 2015, **5**, 1500682.

16 S. H. Hadke, S. Levcenko, S. Lie, C. J. Hages, J. A. Márquez, T. Unold and L. H. Wong, *Adv. Energy Mater.*, 2018, **8**, 1802540.

17 J. Fu, Q. Tian, Z. Zhou, D. Kou, Y. Meng, W. Zhou and S. Wu, *Chem. Mater.*, 2016, **28**, 5821–5828.

18 M. S. Kumar, S. P. Madhusudanan and S. K. Batabyal, *Sol. Energy Mater. Sol. Cells*, 2018, **185**, 287–299.

19 W. Koch and M. C. Holthausen, *A chemist's guide to density functional theory*, Wiley-VCH, 2001.

20 P. P. Sun, D. R. Kripalani, L. C. Bai and K. Zhou, *J. Phys. Chem. C*, 2019, **123**, 12684–12693.

21 P. P. Sun, D. R. Kripalani, M. Hao, W. Chi, W. Li and K. Zhou, *J. Phys. Chem. Lett.*, 2020, **11**, 5234–5240.

22 J. J. Scragg, T. Ericson, T. Kubart, M. Edoff and C. Platzer-Björkman, *Chem. Mater.*, 2011, **23**, 4625–4633.

23 W. Li, J. Chen, H. Cui, F. Liu and X. Hao, *Mater. Lett.*, 2014, **130**, 87–90.

24 S. Zhuk, T. K. S. Wong, M. Petrovic, E. Kymakis, S. S. Hadke, S. Lie, L. H. Wong, P. Sonar, A. Dey, S. Krishnamurthy and G. K. Dalapati, *Sol. RRL*, 2020, 2000293.

25 S. Zhuk, T. K. S. Wong, E. Tyukalova, A. Guchhait, D. H. L. Seng, S. Tripathy, T. I. Wong, M. Sharma, H. Medina and G. K. Dalapati, *Appl. Surf. Sci.*, 2019, **471**, 277–288.

26 S. Zhuk, T. K. Sh. Wong, S. Sudhakar, S. Lie, A. Guchhait, Y. Gao, L. Helena, S. Cheng and X. Wang, *Sol. Energy*, 2019, **194**, 777–787.

27 G. Kresse and J. Furthmüller, *Phys. Rev. B: Condens. Matter Mater. Phys.*, 1996, **54**, 11169.

28 J. P. Perdew, K. Burke and M. Ernzerhof, *Phys. Rev. Lett.*, 1996, **77**, 3865–3868.

29 A. D. Becke, *Phys. Rev. A: At., Mol., Opt. Phys.*, 1988, **38**, 3098.

30 S. R. Hall, J. T. Szymanski and J. M. Stewart, Kesterite, *Can. Mineral.*, 1978, **16**, 131.

31 J. Paier, R. Asahi, A. Nagoya and G. Kresse, *Phys. Rev. B: Condens. Matter Mater. Phys.*, 2009, **79**, 115126.

32 S. Chen, X. G. Gong, A. Walsh and S. H. Wei, *Appl. Phys. Lett.*, 2010, **96**, 021902.

33 A. J. Jacksona and A. Walsh, *J. Mater. Chem. A*, 2014, **2**, 7829–7836.

34 J. Chen, F. Wang, B. Yang, X. Peng, Q. Chen, J. Zou and X. Dou, *Coatings*, 2019, **9**, 130.

35 H. Katagiri, K. Jimbo, W. S. Maw, K. Oishi, M. Yamazaki, H. Araki and A. Takeuchi, *Thin Solid Films*, 2009, **517**, 2455–2460.

36 M. Y. Yeh, P. H. Lei, S. H. Lin and C. D. Yang, *Materials*, 2016, **9**, 526.

37 M. M. I. Sapeli, M. T. Ferdaous, S. A. Shahahmadi, K. Sopian, P. Chelvanathan and N. Amin, *Mater. Lett.*, 2018, **221**, 22–25.

38 S. Zhuk, A. Kushwaha, T. K. S. Wong, S. Masudy-Panah, A. Smirnov and G. K. Dalapati, *Sol. Energy Mater. Sol. Cells*, 2017, **171**, 239–252.

39 A. E. H. Benzetta, M. Abderrezek and M. E. Djeghlal, *Optik*, 2019, **181**, 220–230.